# Kinematic Positioning Inside the Ionosphere

Todd Richert, *Waypoint Consulting Inc.*
February 2003

## ABSTRACT

The effect of the ionosphere on GPS signals has caused considerable problems for GPS users. Traditionally, the ionosphere has been approximated as a thin spherical shell through which the GPS signal must travel. This shell has a specific height and density that determines the magnitude of the ionospheric disturbance on the GPS signal. While this simplification of the problem has sufficed for most terrestrial applications, it is not always adequate.

This paper focuses on the problem of navigating a projectile that is launched from the surface of the Earth and passes through the ionosphere before reaching its apogee and reentering the Earth's atmosphere. Clearly, the thin shell model will not suffice for this problem. In this paper, a method for modeling the vertical structure of the ionosphere is presented. This model is then used to correct GPS observations.

An experiment with a data set from a GPS receiver on a NASA rocket has been conducted. The data is processed using a Kalman filter algorithm. This enables a comparison between the *forward* and *reverse* post-processed solutions. The results of the test indicate that the proposed model reduces the forward/reverse separation of the combined solution. This substantiates that the new method for correcting GPS observations improves the internal consistency of the position solution.

## INTRODUCTION

The purpose of this report is to describe a new methodology for correcting GPS measurements for the effects of the ionosphere. In particular, the report focuses on the ionospheric correction for a very high single-frequency receiver platform (inside the ionosphere) operating in differential mode.

A signal traveling between a GPS satellite and a receiver inside the ionosphere will not experience the full effect of the ionosphere; it will be disturbed only by the portion of the ionosphere between the satellite and receiver. Traditionally, the ionosphere has been modeled as a thin spherical shell [2], [3], [5]. Unfortunately, the spherical shell model does not adequately represent the smoothly varying nature of the ionosphere in the vertical direction for a receiver inside the ionosphere.

After explaining the theory behind this new technique, an experiment with a real data set is described. The method for evaluating the performance is non-trivial since there is no truth trajectory with which to compare the results. Therefore, a scheme for evaluating the effectiveness of the approach is explained and the results are presented.

## SIGNIFICANCE OF THE IONOSPHERE

The ionosphere is a layer of the Earth's upper atmosphere that is composed of charged free electrons. This layer of electrons causes a delay in GPS code measurements and an apparent advance in GPS phase measurements. This phenomenon effectively introduces an unknown bias in the GPS measurement model.

An important property of the ionosphere is that it is dispersive with respect to electromagnetic energy in the L-band. Therefore, the L1 and L2 frequencies experience different magnitudes of disturbance. When dual-frequency measurements are available, this property can be exploited to determine the magnitude of the induced ionospheric error. Equation (1) can be used to calculate the ionospheric error corrupting a GPS signal [6].

$$\Delta_{L1}^{IONO} = \frac{f_{L2}^2}{f_{L2}^2 - f_{L1}^2}\left\{\left[\Phi_{L1} - \frac{f_{L1}}{f_{L2}}\Phi_{L2}\right] - \left[N_{L1} - \frac{f_{L1}}{f_{L2}}N_{L2}\right]\right\} \quad (1)$$

$\Delta_{L1}^{IONO}$ is the ionospheric error on L1 in meters.

$f_{L1}, f_{L2}$ are the L1 and L2 carrier frequencies in Hertz.

$TEC$ is the Total Electron Content in TECU. One TECU is equivalent to $10^{16}$ electrons per square meter along the path of the signal and corresponds to a 16 cm error on L1.

Indirectly, the magnitude of this error provides information about the TEC along the path of the GPS signal. The relationship between TEC and ionospheric error is given by [3]

$$\Delta_{L1}^{IONO} = \frac{40.3}{f_{L1}^2} TEC \quad (2)$$

## MODELING VERTICAL TOTAL ELECTRON CONTENT

The density and height of the ionosphere vary both temporally and spatially. Figure (1) shows the diurnal and vertical variation of electron density for an arbitrary day and location. The data for this figure comes from the International Reference Ionosphere [4].

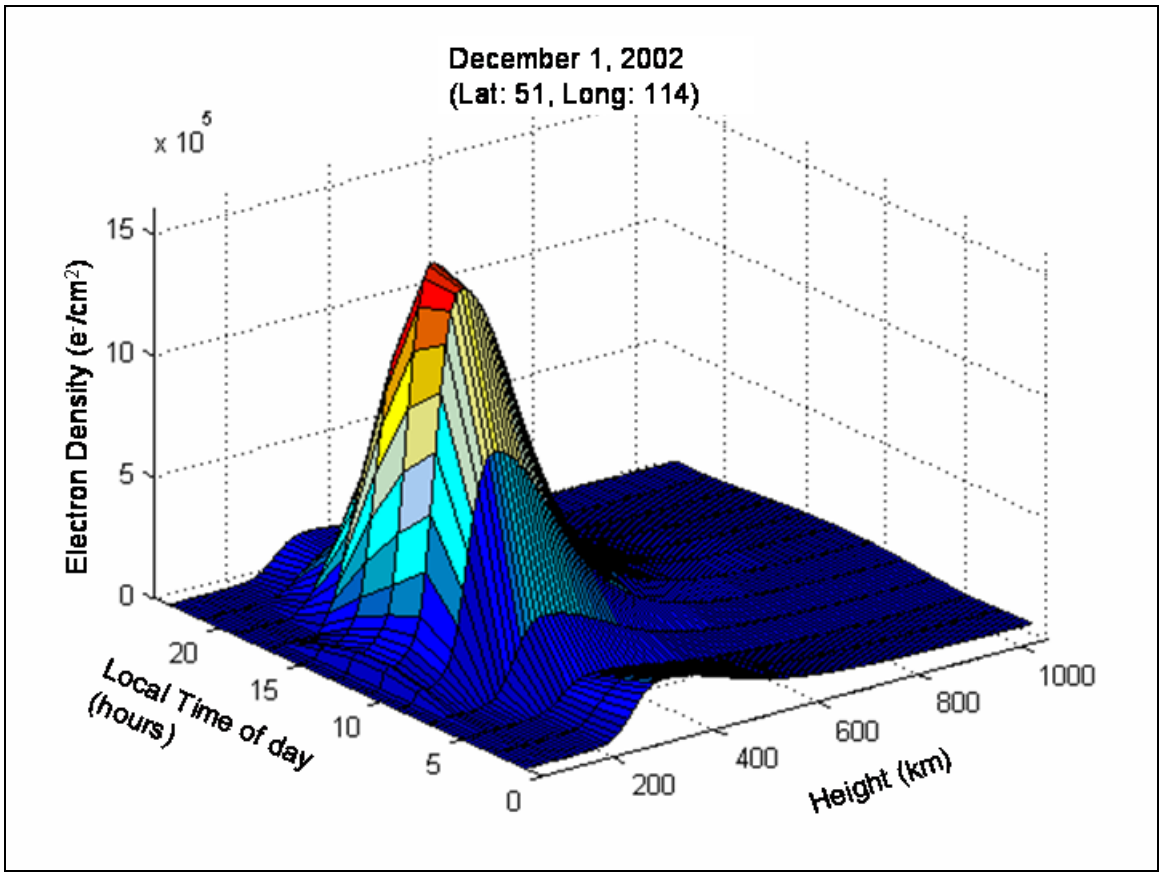


**Figure 1.** Diurnal and vertical variation of electron density.

The following equation can be used to integrate the electron density along the path of a GPS signal [3].

$$TEC = \int_l \rho(l) dl \quad (3)$$

$\rho(l)$ is electron density and $l$ is the length of the path through the ionosphere.

The resulting plot of TEC as a function of time and signal path is shown in figure (2).

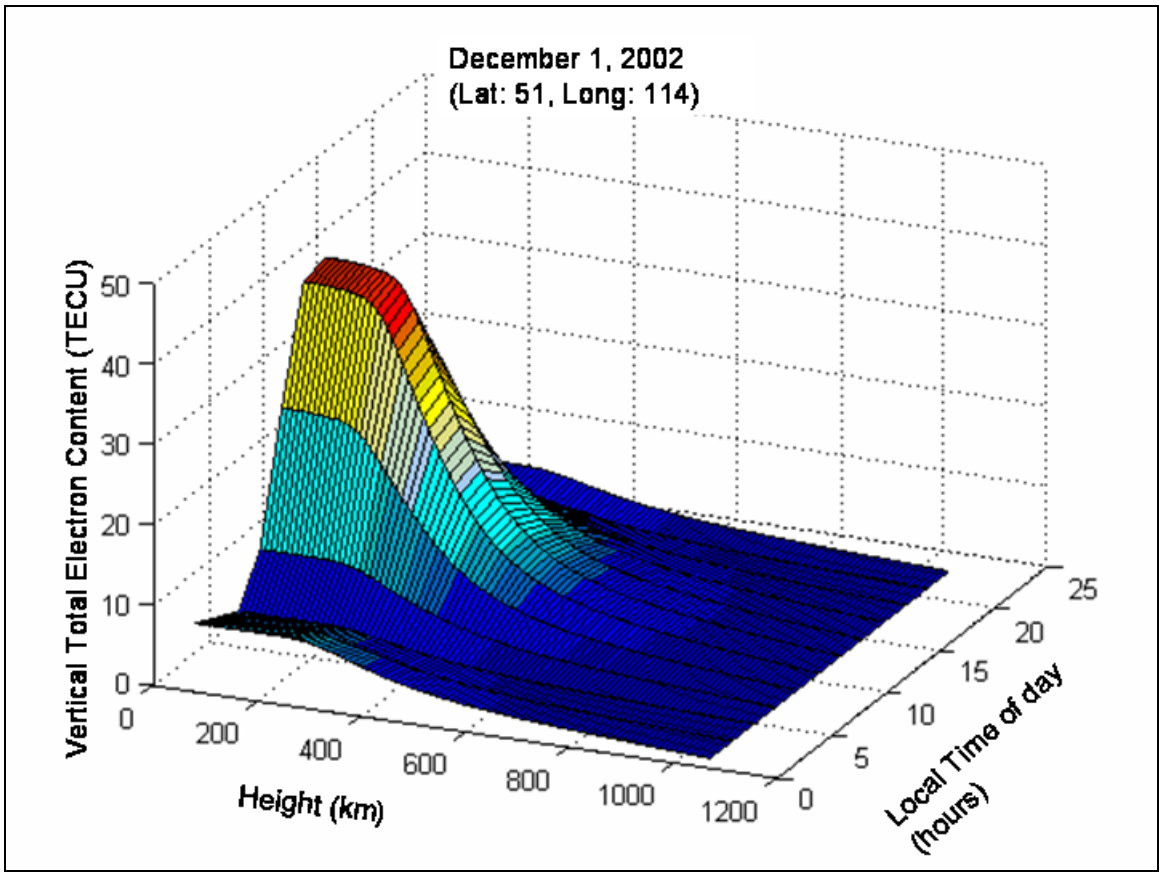


**Figure 2.** Diurnal and vertical variation of TEC.

As expected, the TEC is greatest when the signal path is longest (i.e. when the projectile is below the ionosphere) and decreases exponentially as the signal path decreases.

A two-dimensional representation of this data is shown in figure (3a) where each line represents a different time of day. Figure (3a) reveals that the general shape of the curve is constant over the course of a day. That is, the curvature of the plot is similar for any time while the magnitude varies according to the time of day. Based on this observation, one can create a simple model of the curve that has a constant shape, but is scaled by a varying factor.

In order to model the shape of the curve, plots like figure (3a) were discretized and normalized. To discretize the plot, a sample of times (i.e. every fifteen minutes) and signal lengths (i.e. every twenty kilometers) were chosen and recorded in a lookup table. The normalization process simply involved dividing all values in the lookup table by the largest value. The result is a discrete function of values between zero and one that change as a function of local time (figure (3b)). A representative sample of such lookup

tables was then averaged to produce a local model of the vertical variation of the ionosphere (figure (3c)).

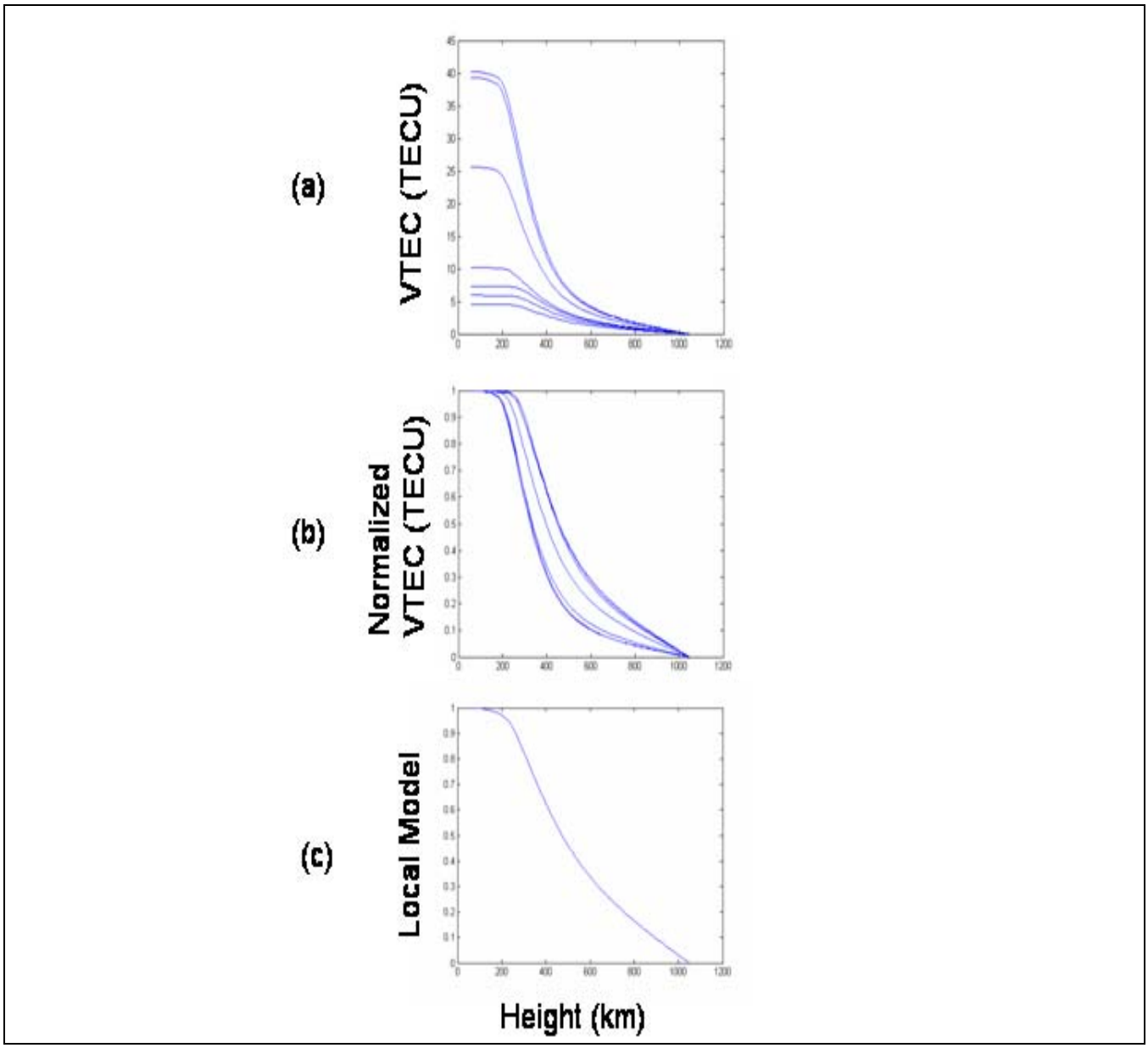


**Figure 3. (a)** Vertical Total Electron Content versus height of the projectile for various times of the day. **(b)** Normalized VTEC versus the height of the projectile for various time of the day. **(c)** A local model of normalized VTEC versus height of the projectile.

## OBSERVATION CORRECTIONS

The lookup table developed in the previous section can be used to correct GPS observations from a projectile traveling inside the ionosphere. The first step is to determine the TEC along the path of the signal as if the projectile were below the

ionosphere. This can be done by applying equation (1) at a nearby base station with a dual-frequency GPS receiver. The assumption is made that the path between the base station and the satellite and the path between the projectile and the satellite are close enough that any horizontal spatial variation of the ionosphere is negligible.

This ionospheric delay can be converted to TEC via equation (2). It is important to note that the TEC derived from equation (2) is the TEC along the path of the GPS signal between the base station and the satellite. In order to apply the correction based on the lookup table, the *vertical* TEC must be known. Therefore, a mapping function based on the satellite-receiver geometry must be used to map the slant TEC to vertical TEC (VTEC). The mapping function used in this experiment is shown in equation (4) [8].

$$VTEC_{base} = TEC_{base} \sqrt{1 - \frac{\cos^2 E_{base}}{(1 + h_m / R_E)^2}} \quad (4)$$

$E_{base}$ is the elevation angle of the base station.

$h_m$ is the mean height of the ionosphere (typically 350 km).

$R_E$ is the average radius of the Earth.

Once the VTEC is known, the lookup table can be used to adjust the ionospheric correction at the projectile according to the height of the projectile. This is done through the application of equation (5).

$$VTEC_{proj} = VTEC_{base} * \varepsilon(h_{proj}) \quad (5)$$

$h_{proj}$ is the height of the projectile.

$\varepsilon(h_{proj})$ is the appropriate scaling factor from the lookup table in figure (3c).

The adjusted value of VTEC from equation (5) must be mapped onto the slant path between the projectile and the satellite using the same mapping function (equation (4)) but substituting the elevation angle from the projectile to the satellite for the elevation angle from the base station to the satellite.

Finally, the TEC along the slant path between the projectile and the satellite can be converted into a range delay though the use of equation (2). This is the adjusted ionospheric correction to be applied to the observations at the projectile.

All the relevant equations for determining the ionospheric correction can be combined into one expression that is shown as equation (6).

$$\Delta_{L1}^{IONO}(proj) = \varepsilon(h_{proj}) * \Delta_{L1}^{IONO}(base) * \left[ \frac{\sqrt{1 - \frac{\cos^2 E_{base}}{(1 + h_m / R_E)^2}}}{\sqrt{1 - \frac{\cos^2 E_{proj}}{(1 + h_m / R_E)^2}}} \right]$$

(6)

## DESCRIPTION OF THE TEST

To test the performance of the ionospheric corrections, real data from a NASA rocket has been analyzed. The rocket was launched at 21:45 on February 10, 1999 from a launch site near Fairbanks, Alaska. In terms of the diurnal cycle, the rocket was launched at a time of low ionospheric activity (see figure (1)). A continuously operating International GPS Service (IGS) station located 137 km from the launch site was used as the base station. The rocket traveled from the surface of the Earth through the ionosphere, reached its apogee above the ionosphere (at a height of 1050 km) and returned through the ionosphere on its way back to the Earth's surface. Figure (4) shows the North, East, and Up components of the vector between the base station and the projectile over time.

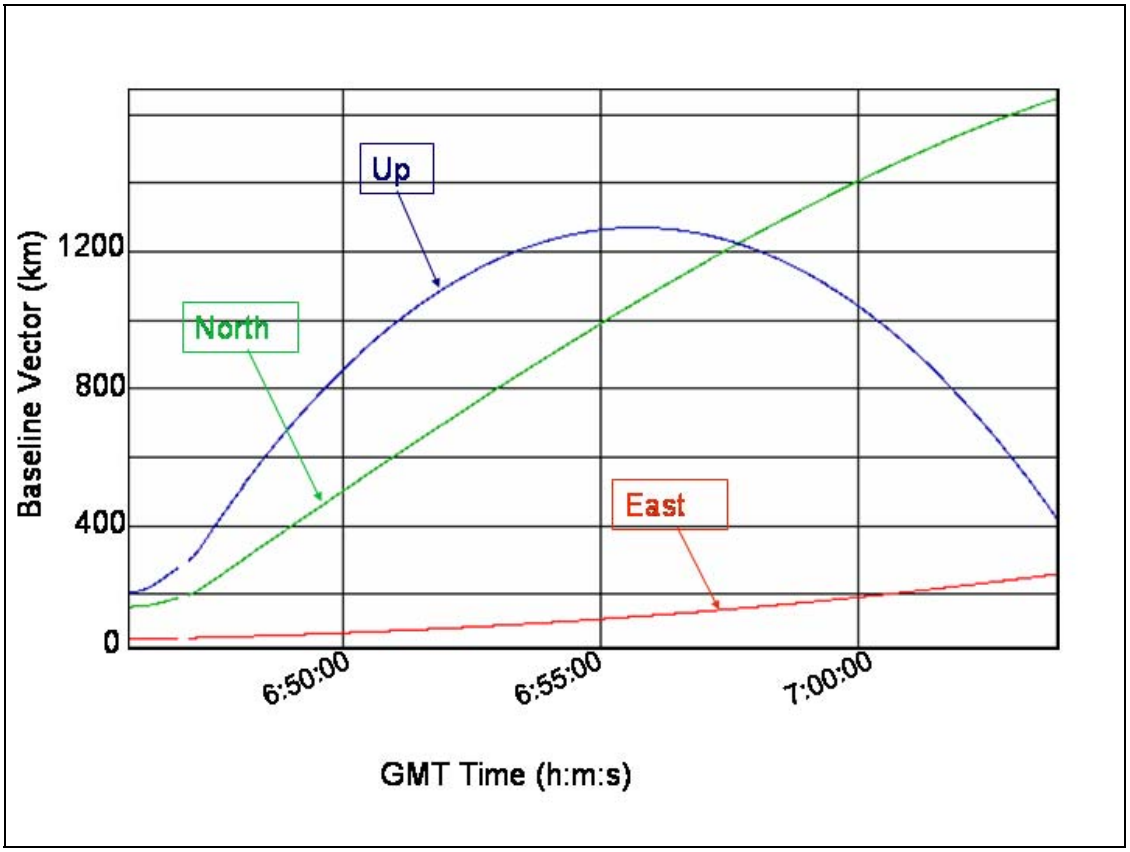

**Figure 4.** North, East, and Up components of the baseline vector.

Applying equation (6) to the rocket data yields a varying ionospheric correction based on the height of the projectile. Figure (5) shows the ionospheric correction for satellite 17 at both the base station and the projectile.

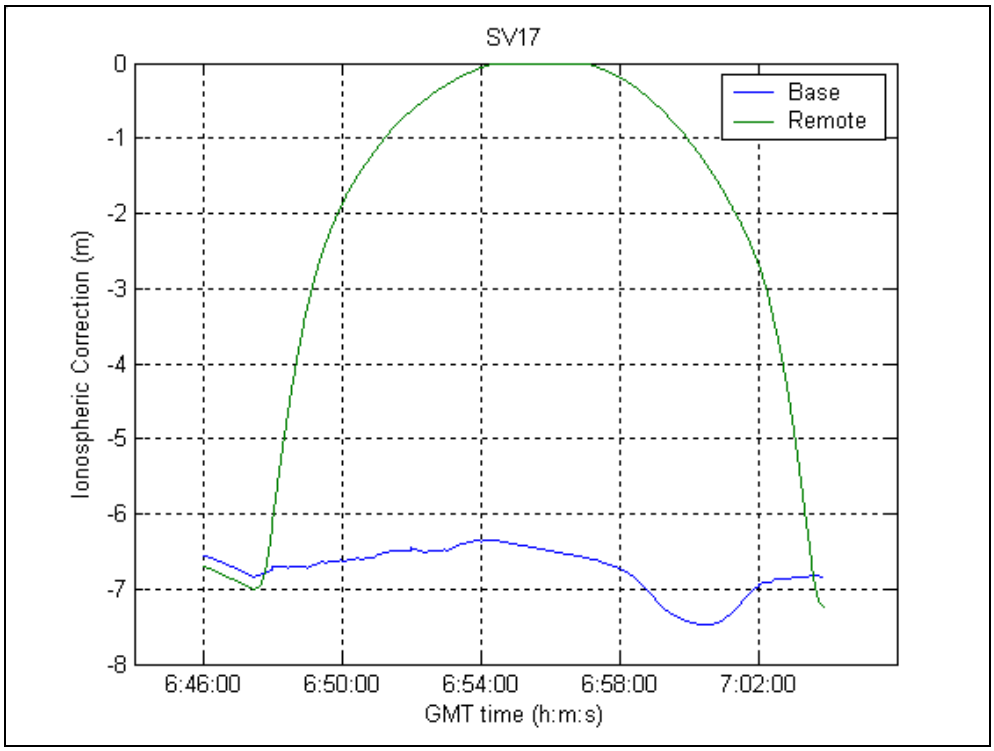


**Figure 5.** Ionospheric correction at the base station and projectile.

As expected, the ionospheric correction diminishes in magnitude as the height of the projectile increases. When the projectile is completely above the ionosphere, the correction is zero.

## PERFORMANCE EVALUATION

An absolute accuracy analysis is not possible because there was no reference trajectory with which to compare the position results. However, the data was processed using GrafNav GPS post-processing software. It is a Kalman filter processor that simultaneously processes carrier phase data and code data to obtain an optimal solution. When using a Kalman filter, one can process the data in the forward and the reverse direction. The separation between the two solutions is an indication of the consistency of the solution. If an ionospheric bias exists in the data, the forward and reverse solutions will converge to a different value of the carrier phase ambiguity term. As a result the forward/reverse separation will be larger. On the other hand, if the ionospheric bias has been effectively removed from the data, the forward and reverse solutions will converge

to the same value of the unknown ambiguity and the forward/reverse separation will be smaller.

This methodology requires that there are no filter resets throughout the data. Filter resets are induced by the software when unfixable carrier phase data is encountered and they will cause a recomputation of the ambiguity including the local ionospheric error. Too many of these resets will cause the separation to be artificially decreased. In addition, if the magnitude of the ionospheric error is the same at the beginning and end of the data, a canceling effect will occur in the uncorrected separation. Hence, little or no improvement will be observed.

**RESULTS**

The following plots show the separation between the forward and reverse solutions. Figure (6) is the raw data that has not been adjusted and figure (7) is the data that has been adjusted with the lookup table. The red, green, and blue lines represent the East, North, and vertical channels respectively.

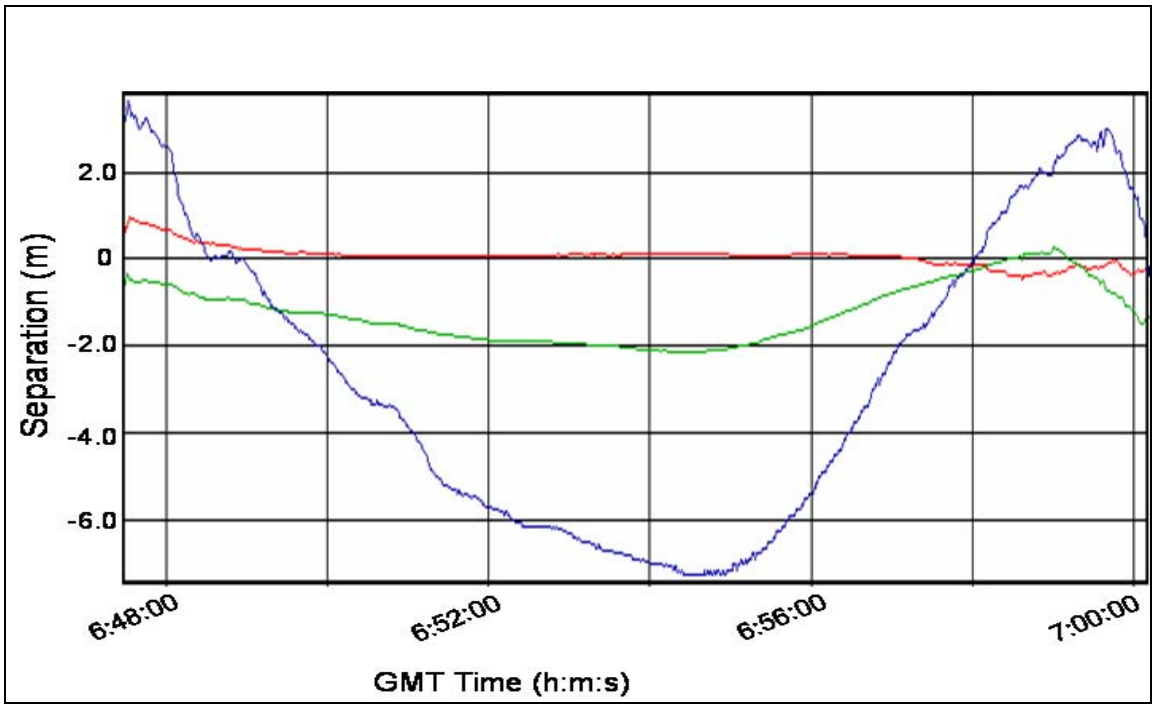


**Figure 6.** Forward/reverse separation for raw data.

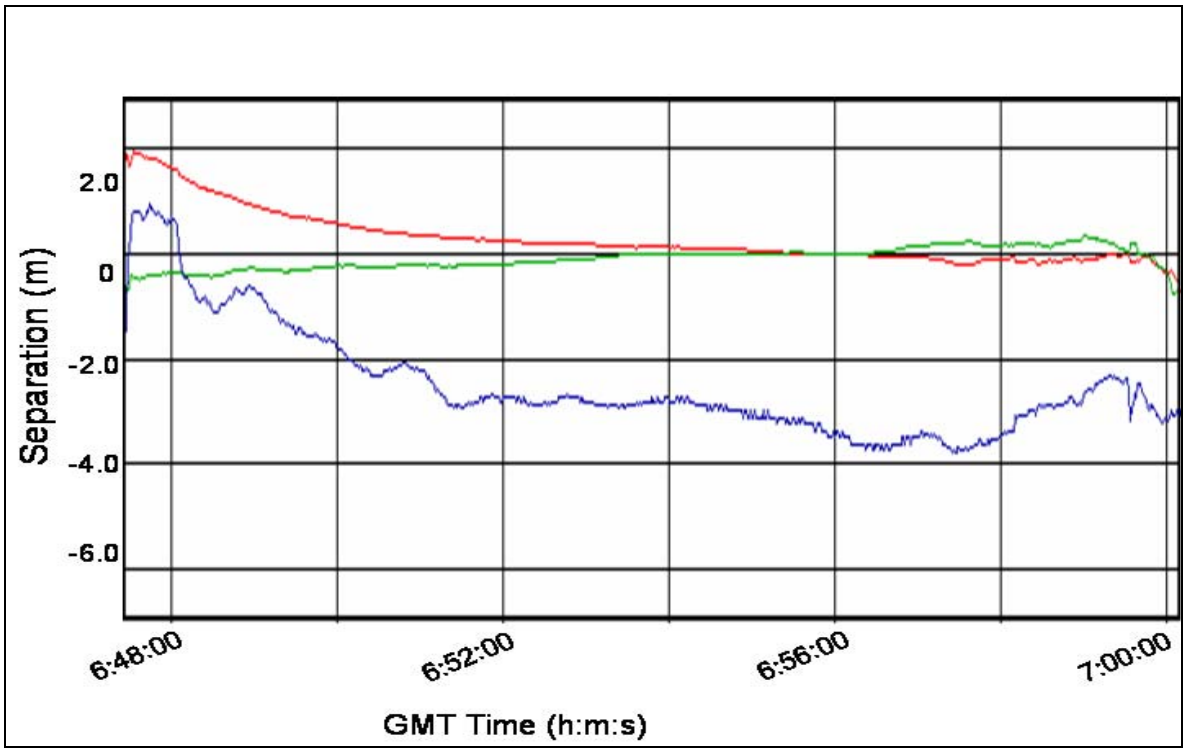


**Figure 7.** Forward/reverse separation for adjusted data.

The root-mean-square (RMS) statistics of the above two plots are given in table 1.

**Table 1.** Plot statistics.

| | | Root-Mean-Square (m) |
|---|---|---|
| Raw data | Horizontal | 1.4 |
| | Vertical | 4.4 |
| Adjusted data | Horizontal | 0.6 |
| | Vertical | 2.7 |

As figures (6) and (7) illustrate, an ionospheric bias predominantly affects the vertical channel. Correspondingly, the improvement resulting from using the lookup table is greatest in the vertical channel (1.7 meters).

Although the vertical channel was significantly improved, it still shows a 2.7 m (RMS) difference, which is much greater than the horizontal channel. This is most likely caused by unmodeled baseline dependent ionospheric errors that are most pronounced in the vertical channel. In figure (4), it can be seen that the projectile travels over 1400 in a northerly direction. Typically, differential ionospheric error is 1-4 ppm, which could easily account for this larger error (eg. 2 ppm of 1400 km is 2.8 m).

## CONCLUSIONS

This paper has described a methodology for adjusting ionospheric corrections for very high receiver platforms according to the height of the platform. The approach given uses a normalized lookup table to describe the vertical consistency of the ionosphere. This information is then used to adjust an ionospheric correction acquired from a nearby base station.

To evaluate the method, a comparison of the forward and reverse Kalman filter solutions is examined. Figures (6) and (7) and table (1) demonstrate that the method reduces the forward/reverse separation in the vertical channel by 1.7 m (RMS) and by 0.8 m (RMS) in the horizontal channel. The remaining errors are accounted for by the baseline dependent ionospheric error. Therefore, it can be concluded that the methodology described in this report improves the concurrence between the forward and reverse solutions.

## FUTURE WORK

In order to expound upon this methodology, more research should be conducted to investigate the use of multiple base stations. Only one base station was used in this experiment, but an improved estimate of the ionospheric correction could be obtained by using two base stations or even a regional network of base stations.

Another recommendation is to launch a rocket with an onboard dual-frequency receiver. The dual-frequency data could be used to totally eliminate the ionospheric bias. The data could then be processed in single frequency mode to evaluate the absolute accuracy of the method.

## ACKNOWLEDGEMENTS

The author would like to express his appreciation to Darren Cosandier and Hugh Martell for their support and to Barton Bull of NASA for the GPS data.

## REFERENCES

[1] Foster, J. C., Quantitative Investigation of Ionospheric Density Gradients at Mid Latitudes, Proceedings of the Institute of Navigation ION 2000 Conference, Jan 2000.
[2] Gao, Y., and Liu, Z. Z., Precise Ionosphere Modeling Using Regional GPS Network Data, *Journal of Global Positioning Systems*, 1, 18-24, 2002.
[3] Hofmann-Wellenhof, B., Lichtenegger, H., and Collins, J., GPS Theory and Practice, Fifth Edition, Springer Wien, New York, 2000.
[4] International Reference ionosphere, http://nssdc.gsfc.nasa.gov/space/model/models/iri.html, Accessed November 2002.
[5] Juan, J., Rius, A., Hernandez-Pajares, M., A Two-Layer Model of the Ionosphere using Global Positioning System data, *Geophysical Research Letters,* 24, 393-396, 1997.

[6] Lachapelle, G. (2002), "ENGO 625 NAVSTAR GPS: Theory and Applications", Department of Geomatics Engineering, University of Calgary, Calgary
[7] University of OULU: Department of Physical Sciences: Ionosphere (Earth's), http://www.oulu.fi/~spaceweb/textbook/ionosphere.html, Accessed October 2002.
[8] Yamamoto, A., Ohta, Y., Okuzawa, T., Tomizawa, I., and Shibata, T., Characteristics of TEC variations observed at Chofu for geomagnetic storms, *Earth Planets Space*, 52, 1073-1076, 2000.